


# Double-core-hole states in CH<sub>3</sub>CN: Pre-edge structures and chemical-shift contributions

Cite as: J. Chem. Phys. **149**, 134313 (2018); <https://doi.org/10.1063/1.5047854>

Submitted: 10 July 2018 . Accepted: 20 September 2018 . Published Online: 05 October 2018

D. Koulentianos, S. Carniato, R. Püttner , G. Goldsztejn, T. Marchenko, O. Travnikova, L. Journal, R. Guillemin, D. Céolin, M. L. M. Rocco , M. N. Piancastelli, R. Feifel, and M. Simon



View Online



Export Citation



CrossMark

## ARTICLES YOU MAY BE INTERESTED IN

[Coulomb explosion imaging of CH<sub>3</sub>I and CH<sub>2</sub>ClI photodissociation dynamics](#)

The Journal of Chemical Physics **149**, 204313 (2018); <https://doi.org/10.1063/1.5041381>

[Perspective: Computational chemistry software and its advancement as illustrated through three grand challenge cases for molecular science](#)

The Journal of Chemical Physics **149**, 180901 (2018); <https://doi.org/10.1063/1.5052551>

[Photoionization of the iodine 3d, 4s, and 4p orbitals in methyl iodide](#)

The Journal of Chemical Physics **149**, 144302 (2018); <https://doi.org/10.1063/1.5035496>

Where in the **world** is AIP Publishing?

*Find out where we are exhibiting next*



## Double-core-hole states in CH<sub>3</sub>CN: Pre-edge structures and chemical-shift contributions

D. Koulentianos,<sup>1,2</sup> S. Carniato,<sup>2</sup> R. Püttner,<sup>3</sup> G. Goldsztejn,<sup>2</sup> T. Marchenko,<sup>2,4</sup>  
 O. Travnikova,<sup>2,4</sup> L. Journal,<sup>2,4</sup> R. Guillemin,<sup>2,4</sup> D. Céolin,<sup>4</sup> M. L. M. Rocco,<sup>5</sup>  
 M. N. Piancastelli,<sup>2,6</sup> R. Feifel,<sup>1</sup> and M. Simon<sup>2,4</sup>

<sup>1</sup>Department of Physics, University of Gothenburg, Origovägen 6B, SE-412 96 Gothenburg, Sweden

<sup>2</sup>Sorbonne Université, CNRS, Laboratoire de Chimie Physique-Matière et Rayonnement, F-75005 Paris Cedex 05, France

<sup>3</sup>Fachbereich Physik, Freie Universität Berlin, Arnimallee 14, D-14195 Berlin, Germany

<sup>4</sup>Synchrotron SOLEIL, L'Orme des Merisiers, Saint-Aubin, BP 48, F-91192 Gif-sur-Yvette Cedex, France

<sup>5</sup>Institute of Chemistry, Federal University of Rio de Janeiro, Rio de Janeiro 21941-909, Brazil

<sup>6</sup>Department of Physics and Astronomy, Uppsala University, Box 516, SE-751 20 Uppsala, Sweden

(Received 10 July 2018; accepted 20 September 2018; published online 5 October 2018)

Spectra reflecting the formation of single-site double-core-hole pre-edge states involving the N 1s and C 1s core levels of acetonitrile have been recorded by means of high-resolution single-channel photoelectron spectroscopy using hard X-ray excitation. The data are interpreted with the aid of *ab initio* quantum chemical calculations, which take into account the direct or conjugate nature of this type of electronic states. Furthermore, the photoelectron spectra of N 1s and C 1s singly core-ionized states have been measured. From these spectra, the chemical shift between the two C 1s<sup>-1</sup> states is estimated. Finally, by utilizing C 1s single and double core-ionization potentials, initial and final state effects for the two inequivalent carbon atoms have been investigated. *Published by AIP Publishing.*  
<https://doi.org/10.1063/1.5047854>

### I. INTRODUCTION

The development of third-generation synchrotron radiation (SR) sources and X-ray free electron lasers (XFELs) enabled the observation of double-core-hole (DCH) states<sup>1–16</sup> at unprecedented ease. DCH states can be formed by simultaneous or sequential excitation and/or removal of two core electrons, as originally discussed by Cederbaum *et al.*<sup>17</sup> for the case of the two core electrons being ejected into the continuum. As was shown in Ref. 17 and subsequently emphasized in more recent theoretical studies,<sup>18–20</sup> the formation of DCH states in molecules is of particular interest due to the properties of these states. Specifically, molecules where both vacancies have been created on one and the same atom, usually referred to as single-site (ss) DCH, exhibit large orbital relaxation effects, as recently investigated by Linusson and co-workers,<sup>11</sup> whilst molecular DCH states where the two vacancies involve two different atomic sites, referred as two-site (ts) DCH, are prone to enhanced chemical shifts in polyatomic molecular systems which comprise the same atomic species in different chemical environments. Both types of DCH states can be formed either by the ejection of the two core electrons, leading to DCH continuum states, or by a simultaneous core-ionization and core-excitation mechanism, resulting in what is referred to as DCH pre-edge states.

Experimental evidence of DCH states had been reported already from the late seventies, in the work of Ågren *et al.*,<sup>21</sup> by recording the X-ray emission spectrum of Ne, after electron impact in the 1s shell. One of the first experimental observations of DCH final states using electron detection was made by

Eland *et al.*<sup>1</sup> By using a time-of-flight (TOF) magnetic bottle electron spectrometer in combination with synchrotron radiation (SR), ss-DCH continuum states of CH<sub>4</sub> and NH<sub>3</sub> were measured along with the decay paths of these states. Using the same experimental technique, Lablanquie *et al.*<sup>2</sup> obtained, around the same time, the ss-DCH continuum states of N<sub>2</sub>, O<sub>2</sub>, CO, and CO<sub>2</sub> and shortly later the ts-DCH continuum states of C<sub>2</sub>H<sub>2</sub>.<sup>3</sup> Following the studies by Eland *et al.* and Lablanquie *et al.*, Mucke *et al.*<sup>4</sup> investigated the formation of DCH states in H<sub>2</sub>O.

Regarding the observation of DCH pre-edge states, which can be achieved by means of multi-electron coincidence spectroscopy, as originally demonstrated in the work of Eland *et al.*,<sup>1</sup> high-resolution single-channel photoelectron spectroscopy has very recently been proven to also be a very efficient technique for detecting this type of DCH states. The enhanced kinetic energy resolution offered by this single-electron spectroscopy technique allows one to measure in great detail which "super-excited" states the system has been promoted to. For instance, the studies of Püttner *et al.*<sup>5</sup> and Goldsztejn *et al.*<sup>6</sup> are two showcases of how high-resolution electron spectroscopy in combination with a detailed fit analysis can be used for the observation of ss-DCH pre-edge states. Reference 5 focused on the formation of 1s<sup>-1</sup>2p<sup>-1</sup>nℓ DCH states in argon, which led to the identification of Rydberg series within different spin multiplicities, converging to the related double-ionization potential (DIP). Reference 6 focused on DCH states in neon of the type 1s<sup>-2</sup>ns, np and the hypersatellite Auger spectrum, which reflects the decay of different types of DCH states was also presented and subsequently assigned in

Ref. 7. Both Refs. 5 and 6 were able to determine the lifetime width of the doubly core-excited states due to the enhanced energy resolution. Using the same technique as in Refs. 5 and 6, Feifel *et al.*<sup>8</sup> obtained molecular ss-DCH pre-edge states of CS<sub>2</sub> and SF<sub>6</sub> involving the different 1s levels, and Koulentianos *et al.*<sup>9</sup> investigated the DCH pre-edge states of HCl involving the 1s and 2p as well as the 1s and 2s inner shells akin to the Ar work of Ref. 5. A comparison of the two complementary experimental techniques mentioned above was given by Carniato *et al.*<sup>10</sup> In Ref. 10, the photon-energy dependence during the formation of ss DCH pre-edge states in CO<sub>2</sub> was studied using both techniques.

Moreover, experimental studies from which dynamical information on DCH states was extracted have recently been published. More specifically, Marchenko *et al.*<sup>22</sup> obtained the topology of the potential energy surface (PES) and the lifetime of the DCH states of CH<sub>3</sub>I, by performing complementary measurements of resonant inelastic X-ray scattering (RIXS) and resonant Auger spectroscopy (RAS). Furthermore, the highly repulsive nature of DCH states leading to ultrafast dissociation has been illustrated by Travnikova *et al.*<sup>23,24</sup> Finally, as was demonstrated by Céolin *et al.*,<sup>25</sup> resonant energy transfer (RET) in SF<sub>6</sub>, due to the fill of an initial S 1s<sup>-1</sup> vacancy by a S 2p electron, can lead to the formation of S 2p<sup>-1</sup> F 1s<sup>-1</sup> ts-DCH continuum states.

In parallel to the SR experiments mentioned above, Berrah *et al.*<sup>12</sup> investigated the formation of ts-DCH continuum states in CO, by using the world's first XFEL, the Linac Coherent Light Source (LCLS) at SLAC. Using the same light source, Salén *et al.*<sup>13</sup> identified the ts-DCH continuum states of N<sub>2</sub>, N<sub>2</sub>O, CO, and CO<sub>2</sub>. In both studies, the creation of a DCH state is favored by the fact that the duration of the X-ray pulses is comparable to the lifetime of the single-core-hole (SCH) state ( $\approx 4$ –8 fs), thus enabling the absorption of several X-ray photons before the Auger decay sets in. In addition, both the studies of Berrah *et al.* and Salén *et al.*<sup>12,13</sup> validated experimentally the concept of enhanced chemical shifts of ts-DCHs.

From a theoretical point of view, the physical mechanisms leading to the formation of ss-DCH pre-edge states, through single photon absorption, can be separated into two processes, referred to, in what follows, as the direct and the conjugate path. In the first case, absorption of a single photon leads to the dipolar ionization of a core electron accompanied by a monopolar excitation (monopolar “shake-up”) of the second core electron. In the second case, absorption of a single photon results in the dipolar excitation of one core electron while the second core electron is ejected into the continuum in the form of a monopolar driven “shake-off” ionization mechanism. Nakano *et al.*<sup>14</sup> measured the ss-DCH pre-edge states of C<sub>2</sub>H<sub>2n</sub> ( $n = 1, 2, 3$ ) molecules and interpreted the experimentally observed structures in terms of direct and conjugate contributions. Subsequently, a theoretical model accounting for these two processes including its application for the interpretation of other experimental spectra was published by Carniato *et al.*<sup>15,16</sup> demonstrating a very good agreement between experiment and theory.<sup>4,6,8</sup>

In the present work, electron spectra associated with the formation of C 1s<sup>-2</sup>V and N 1s<sup>-2</sup>V DCH states of the CH<sub>3</sub>CN

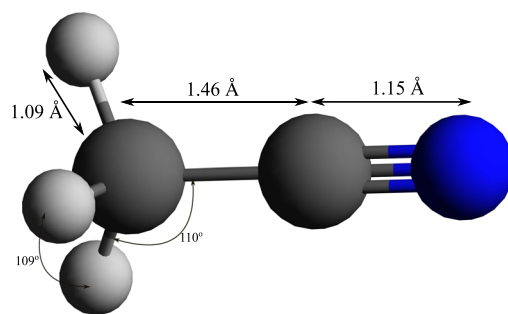


FIG. 1. The CH<sub>3</sub>CN molecule, which comprises a nitrogen atom (blue), two carbon atoms (dark gray), and three hydrogen atoms (light gray). The molecule belongs to the C<sub>3v</sub> point group.

molecule depicted in Fig. 1 have been recorded using the same technique as in Refs. 5, 6, 8, and 9. The interpretation of the experimentally observed structures is again based on numerical calculations, revealing the relative contributions of the direct and conjugate pathway for each transition. Complementary N 1s<sup>-1</sup> and C 1s<sup>-1</sup> photoelectron spectra have also been measured, and from the latter, the chemical shift between the two C atoms has been estimated.

## II. EXPERIMENTAL DETAILS

The experimental work was performed at the GALAXIES beam line of the French national synchrotron radiation facility SOLEIL,<sup>26</sup> Saint Aubin, France. Briefly, the beam line is equipped with two experimental end stations, one of which is fully dedicated to hard X-ray photoelectron spectroscopy (HAXPES)<sup>27</sup> experiments, as employed in the present work. The photons provided by the U20 undulator cover the energy range of 2.3–12 keV. Different photon energies can be selected using a Si (111) double crystal monochromator (DCM) and a collimating mirror, the coating of which can be either palladium or carbon depending on the selected photon energy. Photoelectrons ejected from the target species, which are enclosed in a gas cell, are collected and analyzed with an EW4000 VG Scienta hemispherical analyzer, the electrostatic lens of which is parallel to the electric field vector of the linearly polarized incoming radiation. Energy calibration of the electron spectrometer, for the acquired 1s<sup>-2</sup>V photoelectron spectra, is based on the known LMM Auger spectrum of argon. The binding energy used for calibrating the selected photon energy was 248.63 eV for Ar 2p<sub>3/2</sub><sup>-1</sup>.<sup>28</sup> For more details about the calibration, see Ref. 5. All spectra were measured at a photon energy of 2.3 keV. For the SCH states, a pass energy of 100 eV and for the DCH states, a pass energy of 500 eV were used resulting in a total experimental resolution, including photon bandwidth and spectrometer settings, of 270(10) meV and  $\approx 700$  meV, respectively.

## III. THEORETICAL DETAILS

As previously reported in Refs. 6, 8, 10, and 14–16, in the specific case of 1s<sup>-2</sup>V events, direct and conjugate shake-up processes take place and satellite states of monopolar and dipolar transition nature of the excited electron can be observed with comparable magnitudes. The 1s<sup>-2</sup>V cross sections were





where the SCH lifetimes were taken from Ref. 33 and a Gaussian of 0.6 eV full width at half maximum (FWHM) to simulate the effect of experimental resolution. The influence of the nuclear dynamics on the line shapes has been neglected in the present calculations of the  $1s^{-2}V$  states. A justification for the factor of 3 multiplying the SCH lifetimes can be found in Refs. 6 and 34. In order to estimate with accuracy the absolute energy positions of the most important bands in  $1s^{-2}V$  spectra as well as the N,  $C_{CN}$ , and  $C_{CH_3}$  DCH ionization energies, Density Functional Theory (DFT) calculations have been performed using the Becke three-parameter hybrid exchange<sup>35</sup> and the Lee-Yang-Parr gradient-corrected correlation functional<sup>36</sup> (B3LYP), as implemented in the computational chemistry software General Atomic and Molecular Electronic Structure System [GAMESS(US)].<sup>37</sup> A larger aug-cc-pCVQZ basis set augmented by additional (2s,2p,1d) diffuse orbitals (300 Cartesian Gaussian basis functions) was used.<sup>38</sup>

The results of our calculations are summarized in Tables I and II, where the symmetry of the final states, along with the experimental and theoretical values of binding energy, the square root of mean radius, and Löwdin populations can be found.

#### IV. RESULTS AND DISCUSSION

The interpretation of the experimental spectra is primarily based on the results of the *ab initio* quantum chemical calculations described in Sec. III. To begin with, we note that, due to the nature of the transition in terms of the direct or conjugate pathway, simple arguments can be related to the symmetry of the final states reached. In particular, a monopolar transition within the direct path will be characterised by integrals of the form  $\langle f||i\rangle$ , where  $|i\rangle$  describes the initial  $1s$  orbital and  $|f\rangle$  describes the occupied final state orbital. This overlap integral will be non-zero only if  $|f\rangle$  and  $|i\rangle$  are of the same symmetry. That is, within the  $C_{3v}$  point group, direct transitions will lead to the final states of the form  $1s^{-2}na_1$ , as the symmetry of the initial  $1s$  orbital is of  $a_1$  symmetry.

Similarly, regarding the conjugate path, the dipolar excitation can be described by an integral of the form  $\langle f|D|i\rangle$ , with  $D$  representing the electric dipole moment operator. Again, because of  $a_1$  being the symmetry of the  $1s$  orbital and by considering the products of the form  $\langle f|D_i|a_1\rangle$ , with  $f$  representing all the possible final state orbitals within the given point group, namely,  $a_1$ ,  $a_2$ ,  $e$  and  $D_i$  as the coordinates of the operator, it can be shown that only transitions to orbitals of  $a_1$  and  $e$  symmetries are allowed, whilst transitions of the form  $\langle a_2|D|a_1\rangle$  are forbidden. Thus conjugate transitions will lead to final states of the form  $1s^{-2}na_1$  and  $1s^{-2}ne$ , respectively.

In what follows, we will first briefly discuss the formation of the N  $1s^{-1}$  and C  $1s^{-1}$  SCH states before moving onto the formation of the ss-DCH states involving the same core levels.

##### A. Formation of the N and C $1s^{-1}$ states

Figure 2 shows the N  $1s^{-1}$  and C  $1s^{-1}$  photoelectron spectra of  $CH_3CN$  measured using a photon energy of 2300 eV.

From the spectrum shown in Fig. 2(a), the position of the N  $1s^{-1}$  SCH state in  $CH_3CN$  is located at  $\approx 405.6$  eV

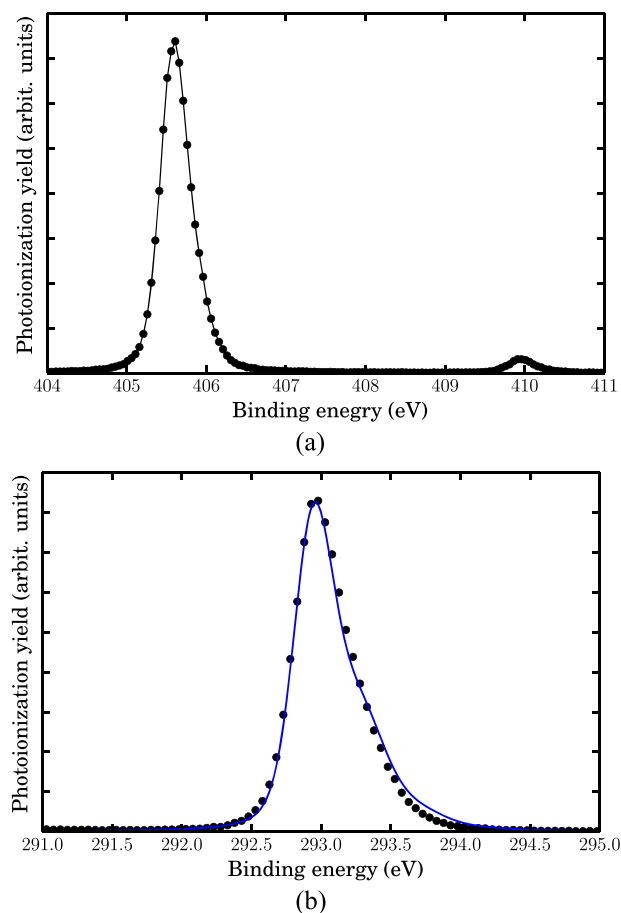


FIG. 2. (a) The N  $1s^{-1}$  photoelectron spectrum and (b) the C  $1s^{-1}$  photoelectron spectrum of  $CH_3CN$ . The blue solid line through the black data points represents the theoretical spectrum convoluted with a Gaussian of 270 meV FWHM in order to simulate the experimental resolution. The good agreement confirms the quality of the theoretical results. Both spectra shown in (a) and (b) were measured at the photon energy of 2300 eV.

and a shake-up has been observed at  $\approx 410$  eV. The value of 405.60(2) eV binding energy measured in the work of Beach *et al.*<sup>39</sup> was used in order to perform the energy calibration of the measured photoelectron spectrum. Moreover, the spectral feature related to the C  $1s^{-1}$  states has been calibrated according to the value of 292.98(7) eV binding energy, measured for the  $CH_3$  carbon site in Ref. 39. Here we have to point out that Beach *et al.* report for the chemically inequivalent  $1s_{CN}^{-1}$  a binding energy of 292.44(8) eV, i.e., a splitting of 0.54(15) eV. This value is larger than the width (FWHM) of the C  $1s^{-1}$  spectral feature shown in Fig. 2(b) of about 500 meV. From this width in combination with the assumption that both carbon atoms possess similar intensities, we can directly conclude that the splitting has to be much smaller than the value given by Beach *et al.* Actually, our theoretical results convoluted with the experimental resolution of 270 meV given in Fig. 2(b) show an excellent agreement with the experimental data. These DFT calculations including vibrational corrections predict binding energies of 292.874 eV and 292.879 eV for the C  $1s_{CN}^{-1}$  and C  $1s_{CH_3}^{-1}$  core holes, respectively, i.e., a splitting of 5 meV. The term vibrational corrections has been used to describe the changes in the vibrational energy levels upon ionization, resulting in a different zero-point energy and subsequent shifts of the  $0 \rightarrow 0$  transition.

## B. Formation of the $N 1s^{-2}V$ states

Figure 3 shows an experimental satellite photoelectron spectrum obtained at the photon energy of 2300 eV which includes the  $N 1s^{-2}V$  states of  $CH_3CN$ , with a direct comparison to a calculated spectrum of this binding energy region.

Five distinct structures are clearly discernible in the experimental spectrum, in particular, three fairly sharp structures which are observed below the  $N 1s^{-2}$  DIP, calculated in the present work to be at 886.61 eV, and two comparatively broad structures which are observed above this threshold. Apart from this, a substantial increase in intensity is apparent close to threshold, reflecting a background, which can be modelled by an arctan function.<sup>5,9</sup> Without going into great details, from a physical point of view, this background is likely to be caused both by transitions to Rydberg states which are very close in energy and hence are difficult to be resolved, as well as excitations to the continuum, i.e., double ionization of the molecule with the ejection of two photoelectrons which can share the available excess energy arbitrarily. The inflection point of this background is expected close to threshold, where the density of the Rydberg states becomes significant. A more detailed description of the origin of this kind of background and its mathematical form can be found in Ref. 40.

Regarding the three peak structures below threshold, the first of them, labeled A, is found to be located at the binding energy  $\cong 872.5$  eV. According to our calculations, this feature is solely due to the conjugate path and corresponds to a transition to the lowest unoccupied molecular orbital (LUMO) of either  $\pi^*$  symmetry if its formation is considered to involve primarily the nitrogen and its neighbouring carbon atom or  $e$  symmetry if the symmetry group of the complete molecule is taken into account. Thus this structure can be assigned as a  $1s^{-2}\pi_{CN}^*(e)$ . Its term value (TV) is  $\cong 15$  eV, which is more than twice the TV of the associated  $1s^{-1}\pi_{CN}^*$  transition, of 5.7 eV, where the latter is based on an estimate from the  $N 1s^{-1}$  inner shell electron energy loss spectrum (ISEELS) of  $CH_3CN$  obtained by Hitchcock *et al.*<sup>41</sup>

The second structure, labeled B, is observed at the binding energy of  $\cong 878.5$  eV. It involves both the conjugate and the direct path, with the latter being dominant as suggested by our numerical investigations. According to our calculations, it involves a transition to a molecular orbital of  $\sigma^*$  symmetry if its formation is considered to involve primarily the nitrogen and the two carbon atoms. By taking the full molecular symmetry into account, we arrive at  $1s^{-2}\sigma_{CCN}^*(a_1)$ . The fact that this peak structure has been recorded below threshold is of particular interest, as its associated structure in SCH studies has been observed well above threshold in the ISEELS spectra<sup>41</sup> and it is referred as the shape resonance. A detailed description of shape resonances has been given by Piancastelli *et al.*<sup>42,43</sup> The TV of this DCH feature is  $\cong 9$  eV suggesting a shift of  $\cong 26$  eV in comparison to the TV of  $-16.9$  eV for the associated  $N 1s^{-1}\sigma_{CN}^*$  feature extracted from the work of Hitchcock *et al.*<sup>41</sup> A similar behavior for the excitations of this kind was already observed in the studies of Feifel *et al.* and Carniato *et al.*<sup>8,16</sup> This substantial shift in energy can be explained by the increased nuclear charge felt by the excited electron in the presence of a double  $1s$  vacancy.

Before moving onto the discussion of the third comparatively strong peak structure, labeled C, we note that our calculations suggest an additional weak structure labeled  $a'$  to be present at  $\cong 880.8$  eV binding energy which seems to be of pure conjugate character. According to our calculations, it can be understood in terms of an excitation to a molecular orbital of  $\sigma^*$  symmetry, if its formation is assumed to primarily involve the two carbons, or in terms of a  $1s^{-2}\sigma_{CC}^*(a_1)$  transition, if the symmetry group of the complete molecule is taken into account. We note that, since we probe the nitrogen site, this feature is expected to be relatively weak and hence more difficult to be discerned in the experimental spectrum in comparison to, for instance, feature C which is clearly observed in the experimental spectrum at the binding energy of  $\cong 882.2$  eV. Again, making use of our calculations, feature C, having an  $a_1$  symmetry, is suggested to be of pure direct nature. On the high binding energy side, feature C is accompanied by another less intense comparatively broad structure labeled D,

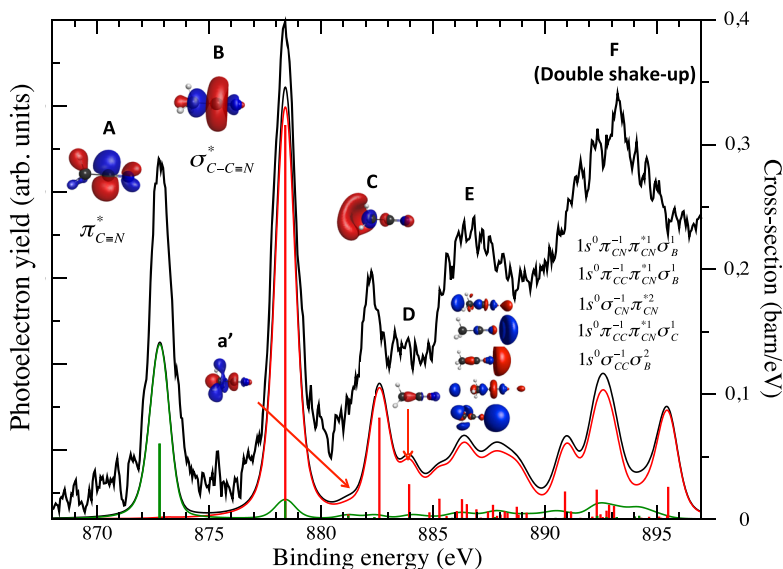


FIG. 3. The experimental satellite photoelectron spectrum, recorded at  $h\nu = 2300$  eV, showing the formation of  $N 1s^{-2}V$  DCH pre-edge states (black line), along with the theoretical spectrum showing the direct (red) and conjugate (green) nature of each transition, as well as the shapes of the MOs of the final states. Peak F consists of several double shake-up transitions. In the assigning of the double shake-up states of peak F,  $\sigma_B$  refers to the  $\sigma_{CCN}^*$  orbital labeled B and  $\sigma_C$  refers to the  $a_1$  type orbital labeled C. The theoretical spectrum has been shifted  $\sim 2.5$  eV toward higher binding energies in order for a clearer comparison between experiment and theory and presentation of our results.

experimentally located at  $\approx 883.7$  eV binding energy. This feature is also of direct nature, but also has a small conjugate character as suggested by our theoretical spectrum. We note that though the states labeled C and D are highly excited and should correspond to ordinary Rydberg states, our calculations indicate that their valence character is non-negligible and therefore they should not be considered as regular atomic-like Rydberg states.

Regarding the two broad structures found close to and above the theoretical core DIP, the first of them is labeled E and located at the binding energy of  $\approx 887$  eV. This peak consists of a number of different transitions for which the most important final state orbitals, being of  $a_1$  symmetry, are depicted in Fig. 3. Though the electron localization of these orbitals substantially exceeds the molecular skeleton, they still have a significant valence character and cannot be considered regular Rydberg states. Most of these highly excited states are located above the N  $1s^{-2}$  DIP, are probably dissociative, and therefore are broad and cannot be resolved individually. Concerning the last comparatively intense structure observed in the experimental spectrum at  $\approx 893$  eV binding energy, our calculations suggest to associate it with the transitions which give rise to region F of the theoretical spectrum, consisting of double shake-up transitions, where the ejection of the photoelectron is accompanied by the simultaneous excitation of two electrons to one or two different unoccupied valence orbitals. For the details of the assignment, see Fig. 3.

### C. Formation of the C $1s^{-2}$ V states

Figure 4 displays an experimental spectrum of acetonitrile in comparison to a numerical spectrum calculated for the same binding energy, which focuses on a region where ss-DCH pre-edge states involving the two chemically inequivalent C  $1s$  core levels are expected. Seven intense sharp peak structures are observed in the experimental spectrum and are very well reproduced by our numerically calculated spectrum.

Before going into details of the interpretation of these peak structures, it should be noted that in the present case, hardly

any background is discernible in the experimental spectrum, in contrast to what was observed for the N  $1s^{-2}$ V case discussed above. This qualitative difference is reminiscent of what was reported before in the DCH pre-edge study of  $\text{SF}_6$  of Feifel *et al.*,<sup>8</sup> where in the case of the F  $1s^{-2}$ V spectrum, a substantial background, which could be modelled by an arctan function, was present, while in the case of the S  $1s^{-2}$ V spectrum, hardly any background was observed. The reason for this type of background being present in some cases while not in others remains a matter of further investigations.

Based on our calculations, the sharp structures can be identified and assigned in terms of DCH pre-edge states involving the CN and  $\text{CH}_3$  sites of acetonitrile. In particular, the first feature, located in the experimental spectrum at the binding energy of  $\approx 637$  eV and labeled A, is associated with the formation of a double core vacancy on the CN site. We assign it to  $1s^{-2}\pi_{\text{CN}}^*(e)$  transitions. As we discussed before, this kind of transition involves the conjugate channel. From the calculated position of the  $1s_{\text{CN}}^{-2}$  threshold at 653.03 eV, the TV for this transition is estimated to be 16.03 eV, which is  $\approx 2.9$  times the TV, of 5.5 eV, obtained for the associated  $1s^{-1}\pi_{\text{CN}}^*$  transition observed by Hitchcock *et al.*<sup>41</sup>

The second structure located at the binding energy of  $\approx 641.5$  eV is found to comprise two different peaks, which correspond to features B and C of the theoretical spectrum, both of which have a direct and a conjugate nature with the former being dominant. In particular, based on our calculations, feature B is related to the formation of a C  $1s^{-2}(a_1)$  state. Furthermore, feature C is related to a final state reached by a transition of the  $1s_{\text{CH}_3}^{-2}\sigma_{\text{CC}}^*(a_1)$  type. From the calculated  $1s_{\text{CH}_3}^{-2}$  threshold at 652.37 eV and the peak position, the TV of this transition is estimated to be 10.87 eV which is  $\approx 5$  times the TV of the associated single core hole  $1s_{\text{CH}_3}^{-1}\sigma_{\text{CC}}^*$  transition.<sup>41</sup> As mentioned above, the increased TVs are due to the high charge seen by the excited electron.

The next sharp structure experimentally observed at the binding energy of  $\approx 644.5$  eV is associated with feature D of the theoretical spectrum. Accordingly, we propose to assign it to a  $1s_{\text{CN}}^{-2}\sigma_{\text{CCN}}^*(a_1)$  transition, which corresponds to the shape resonance in the SCH case. In contrast to the SCH case, the present

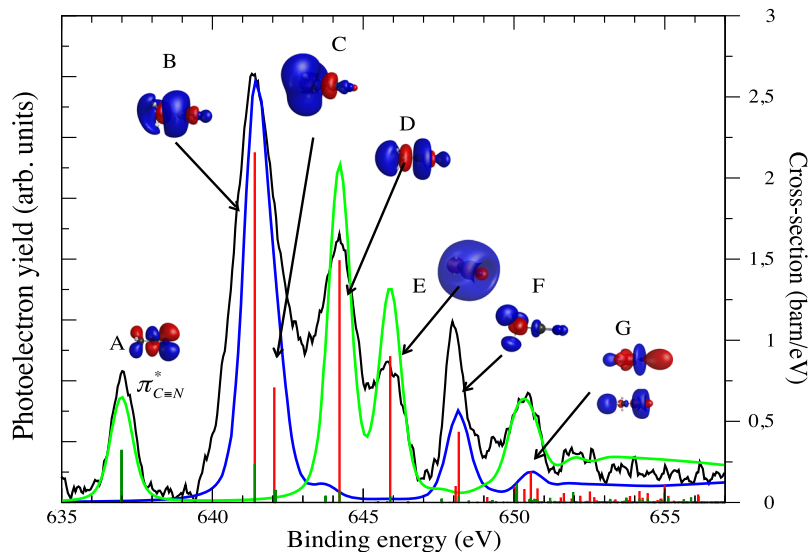


FIG. 4. Experimental satellite photoelectron spectrum, showing the formation of C  $1s^{-2}$ V DCH states, recorded at  $h\nu = 2300$  eV (black line), along with the theoretical spectrum showing the formation of C\*N  $1s^{-2}$ V DCH states (light green line) and C\*H<sub>3</sub>  $1s^{-2}$ V DCH states (blue line). The direct and conjugate character of each transition is also depicted in red and green, respectively. Finally the MOs of the final states can also be seen. The theoretical spectrum has been shifted  $\sim 1.5$  eV toward higher binding energies in order for a clearer comparison between experiment and theory and presentation of our results.

feature is observed below threshold akin to the N 1s case discussed above. In addition, according to theory, the direct and conjugate pathways are likely to interfere for this transition, with the direct channel being again the most intense. The TV of this state is estimated to be about 8.53 eV, which suggests a shift of 24.03 in comparison to the TV of the associated SCH state of  $-15.5$  eV based on estimates from the work of Hitchcock *et al.*<sup>41</sup>

For the three remaining sharp features, labeled in the spectrum as E, F, and G, an assignment in terms of their properties, like the bond character or valence/Rydberg character, is not possible. Therefore, the assignment is restricted to the carbon atom where the DCH is created and to the symmetry character of the excited state orbital. Peak E at a binding energy of  $\approx 646$  eV can be assigned to a C  $1s_{\text{CH}_3}^{-2}(a_1)$  state while peak F at  $\approx 648$  eV is due to a C  $1s_{\text{CN}}^{-2}(a_1)$  state. Finally, peak G at a binding energy of  $\approx 652.5$  eV consists of one C  $1s_{\text{CH}_3}^{-2}(a_1)$  and one C  $1s_{\text{CN}}^{-2}(a_1)$  state. In the case of peak F, the excited electron is mainly localized close to the atoms of the molecule, whereas for the other states under discussion, the excited electron is partially localized far away from the molecular skeleton, i.e., the states have some Rydberg character. The population of these states is mainly caused by the direct shake-up channel.

Finally, from Fig. 4, the enhanced sensitivity of the  $1s^{-2}V$  spectroscopy in probing the environment of an atom in a molecule becomes apparent, as the transitions involving the 1s shells of  $\text{C}_{\text{CN}}$  and  $\text{C}_{\text{CH}_3}$  atoms are well separated. Nevertheless, caution should be exercised, as contrary to the  $1s^{-1}$  or  $1s^{-2}$  states, where the influence of the populated orbitals is reflected in the values of the single and double core-ionization potentials, in  $1s^{-2}V$  measurements is the influence of the unoccupied orbitals, which causes the enhanced sensitivity. Measuring the DIP of the C  $1s^{-1}1s^{-1}$  ts-DCH states of the molecule would allow one to clearly distinguish the two non-equivalent carbon atoms, but this is not possible using our technique. As for C( $1s^{-1}$ )N( $1s^{-1}$ )V ts-DCH, in the present case, it was a too weak channel to be clearly identified. However, the formation of ts-DCH pre-edge states of the form  $1s^{-1}1s^{-1}V$  has been observed for related systems and is the subject of a forthcoming publication.

#### D. Wagner plot and chemical shifts

There are two main effects which cause a change in the core-electron binding energy, i.e., a chemical shift. The first effect is the initial-state shift caused by the charge polarization due to the chemical environment. The second effect is the final-state-relaxation shift, in which the polarizability of the ligands leads to different screening contributions of the core-hole energy. A separation of these two effects is of high interest since it gives, e.g., inside into chemical reactivity, as has been shown in SCH studies performed by Sæthre *et al.*<sup>44</sup> and by Thomas *et al.*<sup>45</sup>

In the following, we shall use the theoretical ionization potentials to investigate these contributions since the performed experiments clearly validate the high accuracy of the present calculations. In our argumentation, including the presentation of Eqs. (1)–(3), we follow Refs. 20 and 50. A similar approach like the one here has also been followed in Ref. 11.

The single ionization potential IP of a  $1s^{-1}$  core hole can be written as

$$\text{IP}(1s^{-1}) = -\epsilon(1s^{-1}) - \text{RC}(1s^{-1}), \quad (1)$$

with  $\epsilon(1s^{-1})$  being the orbital energy and  $\text{RC}(1s^{-1})$  being the relaxation and correlation energy due to the creation of the  $1s^{-1}$  core hole. However, in the case of a chemical shift between two inequivalent carbon atoms, like in acetonitrile, the two contributions of the two individual terms cannot be determined. The separation of these contributions is an application of the DCH states. In previous studies on SCH states,<sup>44,45</sup> initial and final state effects could be corroborated only with the aid of *ab initio* quantum chemical calculations. By knowing the binding energies associated with the formation of SCH and DCH states, a separation between initial and final state effects can in principle be achieved, through a purely experimental approach. For this, the  $1s^{-2}$  double ionization potential DIP has to be written as

$$\begin{aligned} \text{DIP}(1s^{-2}) = & -2 \cdot \epsilon(1s^{-1}) - 2 \cdot \text{RC}(1s^{-1}) \\ & - \text{ERC}(1s^{-2}) + \text{RE}(1s^{-2}), \end{aligned} \quad (2)$$

where  $\text{RE}(1s^{-2})$  is the Coulomb repulsion and  $\text{ERC}(1s^{-2})$  is the excess generalized relaxation energy which represents the non-additive contribution in the DCH relaxation energy. The contributions of the relaxation and correlation effects can be summarized to

$$\text{RC}(1s^{-2}) = \text{ERC}(1s^{-2}) + 2\text{RC}(1s^{-1}). \quad (3)$$

Moreover, for each RC-quantity, the relaxation and correlation contributions can be separated, i.e.,  $\text{RC} = \text{R} + \text{C}$ . It is generally assumed and fully confirmed by the present calculations that the correlation effects are much smaller than the relaxation effects. As a result, Eq. (3) can be approximated by  $\text{R}(1s^{-2}) = \text{ER}(1s^{-2}) + 2\text{R}(1s^{-1})$ . As has been shown from second-order perturbation theory,<sup>17,20</sup>  $\text{ER}(1s^{-2}) = 2\text{R}(1s^{-1})$  and, as a consequence,  $\text{R}(1s^{-2}) = 4\text{R}(1s^{-1})$  can be derived. With these equations and a calculated value for the Coulomb repulsion  $\text{RE}(1s^{-2})$ , which is an atomic quantity and completely independent from the molecular surrounding, one can reconstruct the initial and final state contribution of the chemical shift.

For the core holes of the two inequivalent carbon atoms, the differences of the orbital energies  $\Delta\epsilon$  and the relaxation energies  $\Delta\text{R}$  can be visualized by a Wagner plot, initially discussed by Thomas<sup>46</sup> and used also by Kryzhevoi *et al.*<sup>47</sup> to visualize interatomic relaxation effects in chain molecules upon double core ionization. As can be seen from Fig. 5, in order to draw such a plot, only two quantities are necessary, namely, the DIP and IP, which can both be measured experimentally. From Eqs. (1)–(3), it can be shown that along the blue solid lines, having a slope equal to 3, the orbital energy  $\epsilon$  is constant while along the black dashed lines, having a slope equal to 1, the relaxation energy R is constant. In the following, we use the Wagner plot to visualize the influence of the different approximations on the quantities of interest, namely,  $\Delta\epsilon = \epsilon(1s_{\text{CH}_3}) - \epsilon(1s_{\text{CN}})$  and  $\Delta\text{R} = \text{R}(1s_{\text{CH}_3}) - \text{R}(1s_{\text{CN}})$ . Based on the  $\Delta\text{SCF-HF}$  calculation presented in Table III, the exact values are  $\Delta\epsilon = -0.24$  eV and  $\Delta\text{R} = 0.35$  eV. The values of  $\Delta\epsilon$  and  $\Delta\text{RC}$  along the blue and black dashed lines have been



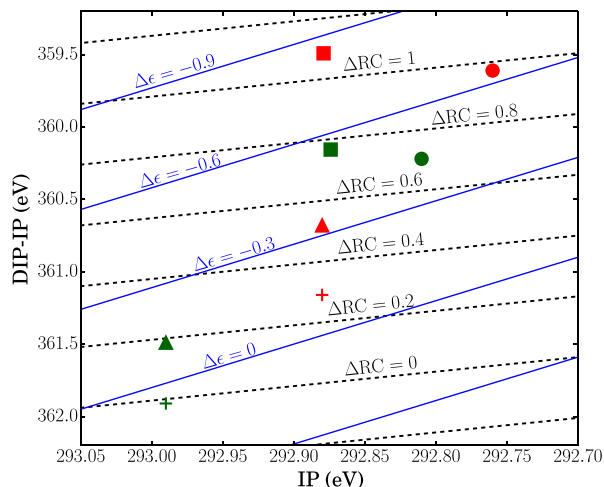


FIG. 5. All points in green refer to the CN carbon atom, whilst points in red refer to the  $\text{CH}_3$  carbon atom. The crosses indicate the values obtained based on the  $\Delta\text{SCF-HF}$  calculations, and the circles are those based on the  $\Delta\text{SCF-DFT}$  calculations. The calculated values for  $\epsilon$ ,  $R(1s^{-1})$ ,  $R(1s^{-2})$ , and  $R(1s^{-2}) = 4R(1s^{-1})$  are indicated by triangles. For the values presented by squares, calculated vibrational corrections have been taken into account for the core-ionized states, whilst for the DCH states, the vibrational corrections were estimated.

set accordingly, in order to illustrate the different values of the orbital energy and the relaxation energy for the two carbon atoms, with respect to the (IP, DIP-IP) points given from theory.

The results for both carbon atoms based on the IP and the DIP calculated with the  $\Delta\text{SCF-HF}$  calculations are indicated with a cross, and  $\Delta\epsilon(\text{HF}) = -0.21$  eV and  $\Delta R(\text{HF}) = 0.32$  eV are obtained. The differences to the exact values given above are due to the fact that  $R(1s^{-2})/R(1s^{-1})$  is 3.97 for both  $\text{CH}_3$  and CN and 3.96 for the N case, which differs slightly from the theoretical value of 4 obtained from second-order perturbation theory.<sup>17,20</sup> To visualize the influence of this deviation, we also calculated the DIP from  $\text{DIP} = -2\epsilon - 4R(1s^{-1}) + \text{RE}(1s^{-2})$ ; the obtained positions in the Wagner plot are indicated by triangles and show a shift to higher DIP-IP values. The positions in the Wagner plot based on the  $\Delta\text{SCF-DFT}$  calculations are shown with circles. From these values,  $\Delta\epsilon(\text{DFT}) = -0.23$  eV and  $\Delta R(\text{DFT}) = 0.28$  eV are derived. The result for  $\Delta\epsilon(\text{DFT})$  is

very close to the exact value of  $-0.24$  eV, which is due to the fact that for both carbon atoms,  $R(1s^{-2})/R(1s^{-1})$  is also very close to 4.

Although we have not determined experimental values for the DIP of  $\text{CH}_3\text{CN}$ , we finally shall discuss the fully experimental approach, i.e., deriving  $\Delta\epsilon$  and  $\Delta R$  based on measured IP and DIP. In this case, vibrational progression has to be taken into account, i.e., the difference of the vibrational zero point energy in the electronic ground and the electronic excited states has to be considered. This value can be different for the inequivalent core holes, as can be seen by the present calculations, since the vibrationally corrected DFT ionization potential of  $1s_{\text{CH}_3}^{-1}$  core-hole state is with  $292.879$  eV  $\times 119$  meV higher than the uncorrected value. For the  $1s_{\text{CN}}^{-1}$  core-hole state, the corrected value of  $292.874$  eV is higher only by 64 meV. Since the vibrational energies and as a result the zero-point energies can both increase and decrease on core ionization (see, e.g., the CO ground state:  $\hbar\omega = 269.0$  meV,<sup>48</sup> C  $1s^{-1}$  state:  $\hbar\omega = 308.7.0$  meV,<sup>49</sup> O  $1s^{-1}$  state:  $\hbar\omega = 230.8$  meV<sup>49</sup>), it is not possible to give a simple estimate for this effect for the double ionization. Because of this, we simply assume for the difference of the zero point energy between the singly core-ionized and the doubly core-ionized state the same absolute value, but with variable size, i.e., between  $-119$  meV and  $119$  meV for  $1s_{\text{CH}_3}$  and  $-64$  meV and  $64$  meV for  $1s_{\text{CN}}$ . The obtained position in the Wagner plot based on the values  $-119$  meV and  $-64$  meV, i.e., by a decrease that fully compensates the first step, is indicated with squares. Generally, the positions in the Wagner plot (not shown here) depend on the exact values chosen for the changes in the zero-point energy, and thus we get  $\Delta\epsilon(\text{DFT}(\text{vib})) = -0.22$  to  $-0.40$  eV and  $\Delta R(\text{DFT}(\text{vib})) = 0.22$ – $0.40$  eV, i.e., values that differ by  $-0.08 \pm 0.09$  eV and  $0.03 \pm 0.09$  eV from the DFT-values without vibrational corrections.

In summary, we conclude that the measured values for the IP and the DIP can cause errors in  $\Delta\epsilon$  and  $\Delta R$ , which can be up to 0.2 eV, due to the influence of the vibrational degrees of freedom. For many molecules, these estimated systematic errors are small compared to the obtained values; see, e.g., Refs. 20, 50, and 51. However, in the present case, such systematic errors are a significant fraction of the obtained results,

TABLE III. Summary of the theoretical ionization energies of the singly and doubly ionized states. Presented are the ionization energies obtained from the  $\Delta\text{SCF-HF}$  and the  $\Delta\text{SCF-DFT}$  calculations as well as the orbital energies  $\epsilon$  and the Coulomb repulsion  $\text{RE}(1s^{-2})$  between the two  $1s$  core holes. From these values, the relaxation energies  $R(1s^{-1})$ , the relaxation and correlation energies  $\text{RC}(1s^{-1})$ , and the correlation energies  $C(1s^{-1})$  for the single core-hole states, as well as the relaxation energies  $R(1s^{-2})$ , the relaxation and correlation energies  $\text{RC}(1s^{-2})$ , and the correlation energies  $C(1s^{-2})$ , the non-additive excess relaxation energies  $\text{ER}(1s^{-2})$ , excess relaxation and correlation energies  $\text{ERC}(1s^{-2})$ , and excess correlation energies  $\text{EC}(1s^{-2})$  for the double core-hole states are given. All values are given in eV.

SCH	$\Delta\text{SCF-HF}$	$\Delta\text{SCF-DFT}$	$\Delta\text{SCF-DFT}(\text{vib. cor.})$	$\epsilon$	$R(1s^{-1})$	$\text{RC}(1s^{-1})$	$C(1s^{-1})$				
C $1s_{\text{CH}_3}^{-1}$	292.88	292.76	292.879	-307.11	14.23	14.35	0.12				
C $1s_{\text{CN}}^{-1}$	292.99	292.81	292.874	-306.87	13.88	14.06	0.18				
N $1s^{-1}$	405.29	405.29	...	-423.64	18.35	18.35	0.00				
DCH				$\text{RE}(1s^{-2})$	$R(1s^{-2})$	$\text{RC}(1s^{-2})$	$C(1s^{-2})$	$\text{ER}(1s^{-2})$	$\text{ERC}(1s^{-2})$	$\text{EC}(1s^{-2})$	
C $1s_{\text{CH}_3}^{-2}$	654.04	652.37	...	96.26	56.44	58.11	1.67	27.98	29.41	1.43	
C $1s_{\text{CN}}^{-2}$	654.90	653.03	...	96.26	55.10	56.97	1.87	27.34	28.85	1.51	
N $1s^{-2}$	887.84	886.61	...	113.25	72.69	73.92	1.23	35.99	37.22	1.23	

due to the small differences in the inequivalent ionization energies. The different approaches provide various values for  $\Delta\epsilon$  and  $\Delta R$ , which are all relatively close to each other, i.e.,  $\Delta\epsilon \cong -0.2$  eV and  $\Delta R \cong 0.3$  eV. We shall now discuss these values.

The fact that the negative orbital energy of the  $C_{CH_3}$  atom is higher than the one for the  $C_{CN}$  atom means that the electron density is lower at the  $C_{CH_3}$  carbon side. This is surprising in the first moment since the  $C_{CH_3}$  atom is bonded to three hydrogen atoms, which have a lower electronegativity and are, therefore, electron donating. In contrast to this, nitrogen has a higher electronegativity and is electron accepting, thus one would expect a shift of the electron cloud toward the N atom, causing a decrease of the electron density at the  $C_{CN}$  side. However, the C–N bond distance is very short, due to the triple-bond character, which in turn increases the charge density at the  $C_{CN}$  side. The higher relaxation energy for an ionization at the carbon bonded to the hydrogen atoms is due to a higher polarizability of the surrounding so that electrons can move more easily toward the carbon atom to screen the created  $1s_{CH_3}^{-1}$  core hole.

## V. CONCLUSION

Photoelectron satellite spectra reflecting the formation of ss-DCH pre-edge states involving the N  $1s^{-2}$  and C  $1s^{-2}$  core levels of acetonitrile have been presented and interpreted based on *ab initio* quantum chemical calculations, taking into account the direct and conjugate nature of this kind of electronic states. Both in the nitrogen and carbon spectra studied, DCH transitions, corresponding to well-known shape resonance features in the SCH case, were found to be located below the DCH ionisation thresholds. Furthermore, a systematic increase of the term value of this kind of DCH states in comparison to their corresponding SCH states was found. Both aspects are suggested to be related to a strong attractive field created by the double core vacancies. Moreover, N  $1s^{-1}$  and C  $1s^{-1}$  photoelectron spectra are reported. The C  $1s^{-1}$  is in line with the theoretically predicted spectrum and reveals a small splitting between the inequivalent core holes. From the theoretical values of the single and double ionization potentials, the initial and final state effects contributing to the chemical shift have been investigated.

## ACKNOWLEDGMENTS

This work has been financially supported by the Swedish Research Council (VR) and the Knut and Alice Wallenberg Foundation, Sweden. D.K. wishes to acknowledge financial support by Labex MiChem, France. The experiments were conducted at the GALAXIES beam line of the synchrotron radiation facility SOLEIL, France (Project No. 99160043), and the authors are grateful to the staff of SOLEIL for the smooth operation of the facility.

<sup>1</sup>J. H. D. Eland, M. Tashiro, P. Linusson, M. Ehara, K. Ueda, and R. Feifel, *Phys. Rev. Lett.* **105**, 213005 (2010).

<sup>2</sup>P. Lablanquie, F. Penent, J. Palaudoux, L. Andric, P. Selles, S. Carniato, K. Bučar, M. Žitnik, M. Huttula, J. H. D. Eland, E. Shigemasa, K. Soejima, Y. Hikosaka, I. H. Suzuki, M. Nakano, and K. Ito, *Phys. Rev. Lett.* **106**, 063003 (2011).

- <sup>3</sup>P. Lablanquie, T. P. Grozdanov, M. Žitnik, S. Carniato, P. Selles, L. Andric, J. Palaudoux, F. Penent, H. Iwayama, E. Shigemasa, Y. Hikosaka, K. Soejima, M. Nakano, I. H. Suzuki, and K. Ito, *Phys. Rev. Lett.* **107**, 193004 (2011).
- <sup>4</sup>M. Mucke, J. H. D. Eland, O. Takahashi, P. Linusson, D. Lebrun, K. Ueda, and R. Feifel, *Chem. Phys. Lett.* **558**, 82 (2013).
- <sup>5</sup>R. Püttner, G. Goldsztejn, D. Céolin, J.-P. Rueff, T. Moreno, R. Kushawaha, T. Marchenko, R. Guillemin, L. Journal, D. W. Lindle, M. N. Piancastelli, and M. Simon, *Phys. Rev. Lett.* **114**, 093001 (2015).
- <sup>6</sup>G. Goldsztejn, T. Marchenko, R. Püttner, L. Journal, R. Guillemin, S. Carniato, P. Selles, O. Travnikova, D. Céolin, A. F. Lago, R. Feifel, P. Lablanquie, M. N. Piancastelli, F. Penent, and M. Simon, *Phys. Rev. Lett.* **117**, 133001 (2016).
- <sup>7</sup>G. Goldsztejn, R. Püttner, L. Journal, R. Guillemin, O. Travnikova, B. Cunha de Miranda, I. Ismail, S. Carniato, P. Selles, D. Céolin, A. F. Lago, R. Feifel, P. Lablanquie, F. Penent, M. N. Piancastelli, M. Simon, and T. Marchenko, *Phys. Rev. A* **96**, 012513 (2017).
- <sup>8</sup>R. Feifel, J. H. D. Eland, S. Carniato, P. Selles, R. Püttner, D. Koulentianos, T. Marchenko, L. Journal, R. Guillemin, G. Goldsztejn, O. Travnikova, I. Ismail, B. Cunha de Miranda, A. F. Lago, D. Céolin, P. Lablanquie, F. Penent, M. N. Piancastelli, and M. Simon, *Sci. Rep.* **7**, 13317 (2017).
- <sup>9</sup>D. Koulentianos, R. Püttner, G. Goldsztejn, T. Marchenko, O. Travnikova, L. Journal, R. Guillemin, D. Céolin, M. N. Piancastelli, M. Simon, and R. Feifel, *Phys. Chem. Chem. Phys.* **20**, 2724 (2018).
- <sup>10</sup>S. Carniato, P. Selles, P. Lablanquie, J. Palaudoux, L. Andric, M. Nakano, Y. Hikosaka, K. Ito, T. Marchenko, O. Travnikova, G. Goldsztejn, L. Journal, R. Guillemin, D. Céolin, M. Simon, M. N. Piancastelli, and F. Penent, *Phys. Rev. A* **94**, 013416 (2016).
- <sup>11</sup>P. Linusson, O. Takahashi, K. Ueda, J. H. D. Eland, and R. Feifel, *Phys. Rev. A* **83**, 022506 (2011).
- <sup>12</sup>N. Berrah, L. Fang, B. Murphy, T. Osipov, K. Ueda, E. Kukk, R. Feifel, P. van der Meulen, P. Salen, H. T. Schmidt, R. D. Thomas, M. Larsson, R. Richter, K. C. Prince, J. D. Bozek, C. Bostedt, S. Wada, M. N. Piancastelli, M. Tashiro, and M. Ehara, *Proc. Natl. Acad. Sci. U. S. A.* **108**, 16912 (2011).
- <sup>13</sup>P. Salén, P. van der Meulen, H. T. Schmidt, R. D. Thomas, M. Larsson, R. Feifel, M. N. Piancastelli, L. Fang, B. Murphy, T. Osipov, N. Berrah, E. Kukk, K. Ueda, J. D. Bozek, C. Bostedt, S. Wada, R. Richter, V. Feyer, and K. C. Prince, *Phys. Rev. Lett.* **108**, 199903 (2012).
- <sup>14</sup>M. Nakano, P. Selles, P. Lablanquie, Y. Hikosaka, F. Penent, E. Shigemasa, K. Ito, and S. Carniato, *Phys. Rev. Lett.* **111**, 123001 (2013).
- <sup>15</sup>S. Carniato, P. Selles, L. Andric, J. Palaudoux, F. Penent, M. Žitnik, K. Bučar, M. Nakano, Y. Hikosaka, K. Ito, and P. Lablanquie, *J. Chem. Phys.* **142**, 014307 (2015).
- <sup>16</sup>S. Carniato, P. Selles, L. Andric, J. Palaudoux, F. Penent, M. Žitnik, K. Bučar, M. Nakano, Y. Hikosaka, K. Ito, and P. Lablanquie, *J. Chem. Phys.* **142**, 014308 (2015).
- <sup>17</sup>L. S. Cederbaum, F. Tarantelli, A. Sgamellotti, and J. Schirmer, *J. Chem. Phys.* **85**, 6513 (1986).
- <sup>18</sup>R. Santra, N. V. Kryzhevoi, and L. S. Cederbaum, *Phys. Rev. Lett.* **103**, 013002 (2009).
- <sup>19</sup>M. Tashiro, M. Ehara, and K. Ueda, *Chem. Phys. Lett.* **496**, 217 (2010).
- <sup>20</sup>M. Tashiro, M. Ehara, H. Fukuzawa, K. Ueda, C. Buth, N. V. Kryzhevoi, and L. S. Cederbaum, *J. Chem. Phys.* **132**, 184302 (2010).
- <sup>21</sup>H. Ågren, J. Nordgren, L. Selander, C. Nordling, and K. Siegbahn, *J. Electron Spectrosc. Relat. Phenom.* **14**, 27 (1978).
- <sup>22</sup>T. Marchenko, G. Goldsztejn, K. Jänkälä, O. Travnikova, L. Journal, R. Guillemin, N. Sisourat, D. Céolin, M. Žitnik, M. Kavčič, K. Bučar, A. Mihelič, B. Cunha de Miranda, I. Ismail, A. F. Lago, F. Gel'mukhanov, R. Püttner, M. N. Piancastelli, and M. Simon, *Phys. Rev. Lett.* **119**, 133001 (2017).
- <sup>23</sup>O. Travnikova, T. Marchenko, G. Goldsztejn, K. Jänkälä, N. Sisourat, S. Carniato, R. Guillemin, L. Journal, D. Céolin, R. Püttner, H. Iwayama, E. Shigemasa, M. N. Piancastelli, and M. Simon, *Phys. Rev. Lett.* **116**, 213001 (2016).
- <sup>24</sup>O. Travnikova, N. Sisourat, T. Marchenko, G. Goldsztejn, R. Guillemin, L. Journal, D. Céolin, I. Ismail, A. F. Lago, R. Püttner, M. N. Piancastelli, and M. Simon, *Phys. Rev. Lett.* **118**, 213001 (2017).
- <sup>25</sup>D. Céolin, J.-P. Rueff, A. Zimin, P. Morin, V. Kimberg, S. Polyutov, H. Ågren, and F. Gel'mukhanov, *J. Phys. Chem. Lett.* **8**, 2730 (2017).
- <sup>26</sup>J.-P. Rueff, J. M. Ablett, D. Céolin, D. Prieur, Th. Moreno, V. Balédent, B. Lassalle-Kaiser, J. E. Rault, M. Simon, and A. Shukla, *J. Synchrotron Radiat.* **22**, 175 (2015).

- <sup>27</sup>D. Céolin, J. M. Ablett, D. Prieur, T. Moreno, J.-P. Rueff, T. Marchenko, L. Journel, R. Guillemin, B. Pilette, T. Marin, and M. Simon, *J. Electron Spectrosc. Relat. Phenom.* **190**, 188 (2013).
- <sup>28</sup>G. C. King, M. Tronc, F. H. Read, and R. C. Bradford, *J. Phys. B: At. Mol. Phys.* **10**, 2479 (1977).
- <sup>29</sup>*Theory and Application of Moment Methods in Many-Fermions Systems*, edited by P. W. Langhoff, B. J. Dalton, S. M. Grimes, J. P. Vary, and S. A. Williams (Plenum, New-York, 1980), p. 191.
- <sup>30</sup>I. Cacelli, V. Carravetta, and A. Rizzo, in *Modern Techniques in Computational Chemistry: MOTECC-91*, edited by E. Clementi (Escom, Leiden, 1991), p. 695 and references therein.
- <sup>31</sup>H. Ågren, V. Carravetta, O. Vahtras, and L. G. M. Pettersson, *Theor. Chem. Acc.* **97**, 14 (1997).
- <sup>32</sup>D. E. Woon and T. H. Dunning, *J. Chem. Phys.* **98**, 1358 (1993).
- <sup>33</sup>C. Nicolas and C. Miron, *J. Electron Spectrosc. Relat. Phenom.* **185**, 267 (2012).
- <sup>34</sup>M. Žitnik, R. Püttner, G. Goldsztejn, K. Bučar, M. Kavčič, A. Mihelič, T. Marchenko, R. Guillemin, L. Journel, O. Travnikova, D. Céolin, M. N. Piancastelli, and M. Simon, *Phys. Rev. A* **93**, 021401(R) (2016).
- <sup>35</sup>A. D. Becke, *J. Chem. Phys.* **98**, 5648 (1993).
- <sup>36</sup>C. Lee, W. Yang, and R. G. Parr, *Phys. Rev. A* **38**, 3098 (1988).
- <sup>37</sup>M. W. Schmidt *et al.*, *J. Comput. Chem.* **14**, 1347 (1993).
- <sup>38</sup>D. E. Woon and T. H. Dunning, Jr., *J. Chem. Phys.* **103**, 4572 (1995).
- <sup>39</sup>D. B. Beach, C. J. Eyermann, S. P. Smit, S. F. Xiang, and W. L. Jolly, *J. Am. Chem. Soc.* **106**, 536 (1984).
- <sup>40</sup>*NEXAFS Spectroscopy*, §7.3, edited by J. Stöhr (Springer Series in Surface Science, 1992).
- <sup>41</sup>A. P. Hitchcock, M. Tronc, and A. Modelli, *J. Phys. Chem.* **93**, 3068 (1989).
- <sup>42</sup>M. N. Piancastelli, D. W. Lindle, T. A. Ferrett, and D. A. Shirley, *J. Chem. Phys.* **86**, 2765 (1987).
- <sup>43</sup>M. N. Piancastelli, *J. Electron Spectrosc. Relat. Phenom.* **100**, 167 (1999).
- <sup>44</sup>L. J. Sæthre, N. Berrah, J. D. Bozek, K. J. Børve, T. X. Carroll, E. Kukk, G. L. Gard, R. Winter, and T. D. Thomas, *J. Am. Chem. Soc.* **123**, 10729 (2001).
- <sup>45</sup>T. D. Thomas, K. J. Børve, M. Gundersen, and E. Kukk, *J. Phys. Chem. A* **109**, 5085 (2005).
- <sup>46</sup>T. D. Thomas, *J. Phys. Chem. A* **116**, 3856 (2012).
- <sup>47</sup>N. Kryzhevoi, M. Tashiro, M. Ehara, and L. S. Cederbaum, *J. Chem. Phys.* **137**, 154316 (2012).
- <sup>48</sup>*Molecular Spectra and Molecular Structure, Vol. I: Spectra of Diatomic Molecules*, edited by G. Herzberg (Van Nostrand Reinhold, New York, 1979).
- <sup>49</sup>R. Püttner, X.-J. Liu, H. Fukuzawa, T. Tanaka, M. Hoshino, H. Tanaka, J. Harries, Y. Tameroni, V. Carravetta, and K. Ueda, *Chem. Phys. Lett.* **445**, 6 (2007).
- <sup>50</sup>O. Takahashi, M. Tashiro, M. Ehara, K. Yamasaki, and K. Ueda, *J. Phys. Chem. A* **115**, 12070 (2011).
- <sup>51</sup>K. Ueda and O. Takahashi, *J. Electron Spectrosc. Relat. Phenom.* **185**, 301 (2012).